

*Original Research Article*

# Recycling of Plastic Waste Made of Polystyrene and Its Transformation into Nanocomposites by Green Methods

Zeyad Zaid Almarbd\*, Nada Mutter Abbass

*Department of Chemistry, College of Science, Baghdad University, Baghdad, Iraq*

## ARTICLE INFO

### Article history

Submitted: 2022-06-29

Revised: 2022-07-02

Accepted: 2021-09-03

Manuscript ID: CHEMM-2208-1603

Checked for Plagiarism: Yes

Language Editor:

Dr. Ermia Aghaie

Editor who approved publication:

Dr. Zeinab Arzehgar

DOI:10.22034/CHEMM.2022.359620.1603

## KEY WORDS

Plystyrene

Graphene oxide

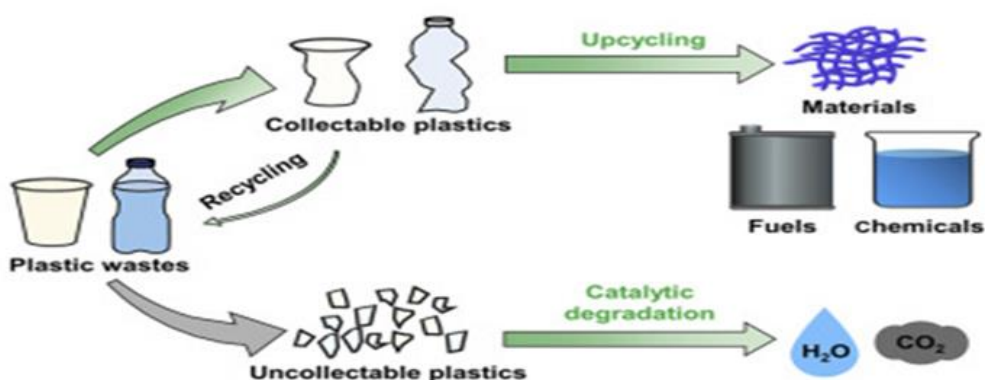
CuO

TiO<sub>2</sub> metal oxide nanoparticles

## ABSTRACT

The titanium dioxide nanoparticles were synthesized by the sol-gel method, while the copper oxide nanoparticles (CuO) were synthesized by the green method by using Sidr extract. The nanocomposites were prepared from the condensation reaction of polystyrene (PS), TiO<sub>2</sub>, CuO, and (GO) by simple mixing method. These structure (PS/GO/CuO) and (PS/TiO<sub>2</sub>/CuO) were characterized by FE-SEM, X-rays diffraction, and thermal analysis. The measurements showed that PS/TiO<sub>2</sub>/CuO and PS/GO/CuO of the synthesized were present in nanoparticle size within the nano-scale. The nanocomposites were tested in the applications of biological activity as antibacterial, antifungal, and antioxidant. The results showed that the nanocomposites (PS/GO/CuO) gave a higher inhibition value than (PS/TiO<sub>2</sub>/CuO) nanocomposites with bacteria.

## GRAPHICAL ABSTRACT



\* Corresponding author: Zeyad Zaid Almarbd

✉ E-mail: [zezozeyad37@gmail.com](mailto:zezozeyad37@gmail.com)

© 2022 by SPC (Sami Publishing Company)

## Introduction

Nanotechnology is one of encouraging development in the current century. The benefit of nanoscience is the ability to transform this science into valuable applications through noticing, control, measurement, and assembly within the nanoscale. In another definition, nanotechnology is a science, technology, and engineering taking place within the nanoscale, it also has applications in all fields of physics, chemistry, medicine, electronics, etc. [1].

Polystyrene is one of the polymers made from its small units of (styrene)  $(C_8H_8)_n$  and has a high molecular weight. Polystyrene can be foamed or solid, whilst the monomer styrene is liquid and its non-expansive resin each for unit weight. In addition, polystyrene form a rather poor barrier with water vapor, oxygen, and low melting point [2].

The study of polymer nano composites are creating widely interesting because of their important applications in domestic uses like memory, electronics, and recording head. It causes a change in the physical properties of polymer and implementing novel features for polymer matrix when adding inorganic nanoparticles to the polymers [3].

The oxides of some metallic nanoparticles, such as  $ZnO$ ,  $Fe_3O_4$ ,  $TiO_2$ ,  $CuO$ , and  $CuO$  are among highly production nanoparticles, so their applications are very wide and utilized as fillers for polystyrene structure, because of their electrical, optical, chemical, and antibacterial properties. As instance, titanium dioxide is low cost and nontoxic material with novel photo catalytic and electrochemical properties generally used the field of chemical fiber production and the UV-resistant material [4].

The NPs green synthesis is an environmentally friendly bio reduction method that does not require the high activation energy needed for the synthesis process. This method has been widely used in the nanomaterial preparation, especially for metal oxides such as actinomycetes and prokaryotic bacteria. Many intracellular proteins and enzymes act as reducing agents for nanoparticle synthesis. Likewise, the other underlying biological agents are plant extracts

which are an alternative to conventional processes for preparing nanometal oxides which are inexpensive, simple, and effective. Plant extracts contain biomolecules like proteins, coenzymes, and carbohydrates, which have the ability to reduce mineral salts to nanoparticles [5].

## Materials and Methods

Scanning Electron Microscope (SEM) by using MIRA3 TESCAN: at Taban laboratory/ Iran, Build 20. Transmission Electron Microscope (TEM) by using FEI Tecnai F20, TF30, JEOL JEM 2100F, FEI Talos F200X: at Taban laboratory/ Iran. X-Ray diffraction (XRD) recorded on Philips PW 1730 portable in PANalytical center/ Iran, 021/44862778. The DSC analyses were measured by using model SDT Q600 V20.9 Differential Scanning Calorimetry at Taban laboratory/ Iran, Build 20. Thermal gravimetric analysis and differential scanning calorimetry were measured by using model SDT Q600 V20.9 at Taban laboratory/ Iran, Build 20. Magnetic stirrer faithful china at the University of Baghdad/College of Science/Department of Chemistry Ultrasonic lab disrupter BIOBASE UCD-150 at the University of Al-Mustansiriyah/College of Science. Furnace gallenkamp muffle furnace at the University of Baghdad/College of Science/Department of Chemistry ([Table 1](#)).

### *Preparation of Sider leaves aqueous extract*

A solution of plant extract of Sidr leaves was prepared with a weight of 4 g of plant extract, 150 mL of distilled water was added to it, and then it was heated for 20 minutes to filter the components in the last step [6].

### *Synthesis of metal oxides nanoparticles*

#### *Copper oxide nanoparticles (Green method) [7]*

4 g of Sidr leaf extract was taken; 100 mL of distilled water was added and heated at 80 °C for 15 minutes, after which the solution was filtered. 6 g of copper(II) sulphate pentahydrate ( $CuSO_4 \cdot 5H_2O$ ) was taken and added deionized water to a volume of 250 mL, and then it was heated at 80 °C with stirring for 15 minutes. Sidr leaf extract was added dropwise to  $CuSO_4 \cdot 5H_2O$  solution with stirring, and then the color was

changed to green and deep green. The mixture was heated at 100 °C until all solvent was evaporated. The solution is dried at 60 °C to obtain the

precipitate, and then it was calcinated at 400 °C until it became blackish-brown color.

**Table 1:** The used chemicals materials

Ser.	Name	Chemical formula	Purity %	Company
1	Copper(II) sulphate pentahydrate	CuSO <sub>4</sub> .5H <sub>2</sub> O	99.5	CDH
2	Titanium isopropoxide	C <sub>12</sub> H <sub>28</sub> O <sub>4</sub> Ti	97	Sigma-Aldrich
3	Sodium nitrate	NaNO <sub>2</sub>	98	CDH
4	Potassium permanganate	KMnO <sub>4</sub>	99.5	CDH
5	Ammonium Hydroxide	NH <sub>4</sub> OH	99	Sigma-Aldrich
6	Sulfuric acid (con.)	H <sub>2</sub> SO <sub>4</sub>	98	Sigma-Aldrich
7	Carbon tetra chloride	CCl <sub>4</sub>	98	
8	Graphite	Graphite	98.2	Fasco expoxies
9	Hydrogen peroxide	H <sub>2</sub> O <sub>2</sub>	97	Sigma-aldrich
10	Hydrochloric acid (con.)	HCl	36.5	Sigma-aldrich
11	Ziziphus spina-christi Leaf extract	leaf extracts		Natural

### Synthesis of TiO<sub>2</sub> nanoparticles [8]

Titanium isopropoxide (10 mL) was dissolved in 100 mL of sider leaves aqueous extract. The mixture was heated at 100 °C for two hours. Yellowish precipitate was found which was then calcined at 350 °C for 2 hours to afford TiO<sub>2</sub> NPs.

### Synthesis of graphene oxide nanoparticles (Hummers' method) [9]

1 g of graphite was added very slowly to cool 50 mL of concentrated H<sub>2</sub>SO<sub>4</sub> and it was stirred in an ice bath for 15 minutes. 4 g of sodium nitrate (NaNO<sub>2</sub>) was added to 6 g of potassium permanganate (KMnO<sub>4</sub>) to the solution and it was stirred in an ice bath (6 hours). The ice bath was removed and the temperature of the mixture was kept at 35 °C in water path (30 minutes). The mixture became deep red- brown color. 50 mL of deionized water was added to the mixture (in step 4). The temperature was increased to 90- 98 °C, then, the above mixture (in step 5) was diluted by adding 250 mL warm deionized water. 20 mL of H<sub>2</sub>O<sub>2</sub> was added until the mixture turned to bright yellow. The mixture is left for 24 hours, after which the washing process is carried out (to get rid of the acids) until the pH reached 7. The graphite oxide (GO) powder was dried at 40 °C (24 hours).

### Synthesis of nanocomposites

#### Synthesis of (Polystyrene/TiO<sub>2</sub>/CuO) nanocomposites [10]

25 mL of carbon tetra chloride (CCl<sub>4</sub>) was added to 1 g of polystyrene and it was refluxed for 1 hour at 50 °C (solution A). 0.1 g of TiO<sub>2</sub> NPs and 0.1 g of CuO NPs were mixed in 10 mL of CCl<sub>4</sub>, and then the mixture was put in ultrasonic for 5 minute (solution B). Solution B was added to solution A, and then it was refluxed for 5 hours. The mixture was collected and left at room temperature until solidified.

#### Synthesis of (Polystyrene/GO/CuO) nanocomposites [10]

25 mL of CCl<sub>4</sub> was added to 1 g of polystyrene, and then it was refluxed for 1 hour at 50 °C (solution A). 0.1 g of GO NPs and 0.1 g of CuO NPs were mixed in 10 mL of CCl<sub>4</sub>, and then the mixture put in ultrasonic for 10 minutes. (solution B). The solution B was added to the solution A and refluxed for 5 hours. The mixture was collected and left at room temperature until solidified.

### Antibacterial activity

Two types of bacteria were selected, they are Gram-negative (*Klebsiella pneumoniae*) and Gram-positive (*Staphylococcus aureus*). The bacterial culture process was carried out in a bacterial medium called (Muller Hinton agar). The utilized

method is called (well diffusion methods) as follow:

The bacterial culture was prepared by 0.1 mL of  $10^6$  CFU/mL broth (liquid medium for culture of bacteria) of indicator strain on the full surface of nutrient agar plate. Three holes were in all the previously prepared agars, the size of each hole was 6 mm. Then, 100  $\mu$ L of 10 M of the sample (the used solvent was DMSO to prepared all samples) to be studied are injected by micropipette for antibacterial activity. Bacterial cultures were incubated at 37 °C for 24 hours, and then the inhibition areas are measured for all compounds [11].

## Results and Discussion

### X-Ray diffraction of PS/TiO<sub>2</sub>/CuO nanocomposites

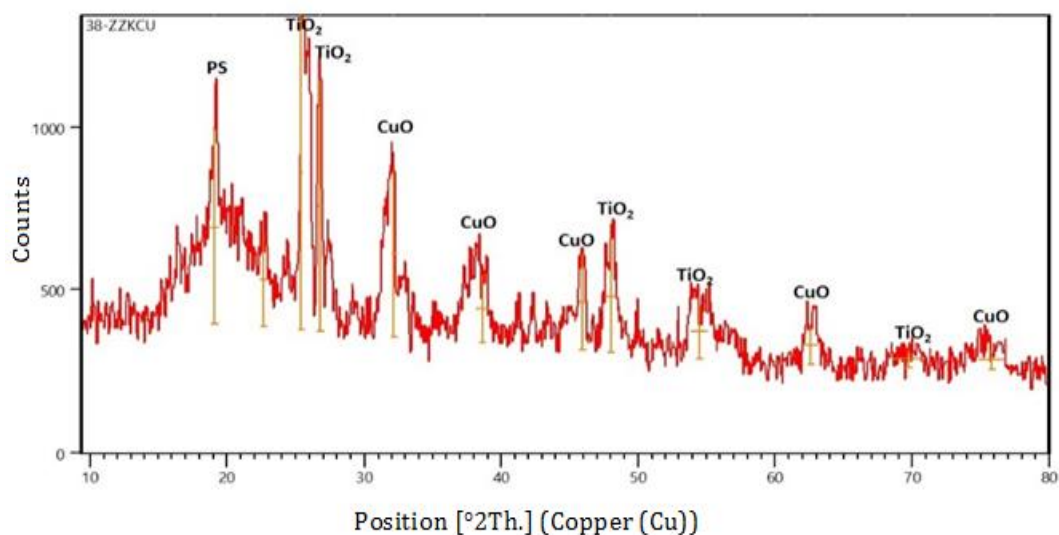


**Figure 1:** XRD pattern of PS/TiO<sub>2</sub>/CuO nanocomposites

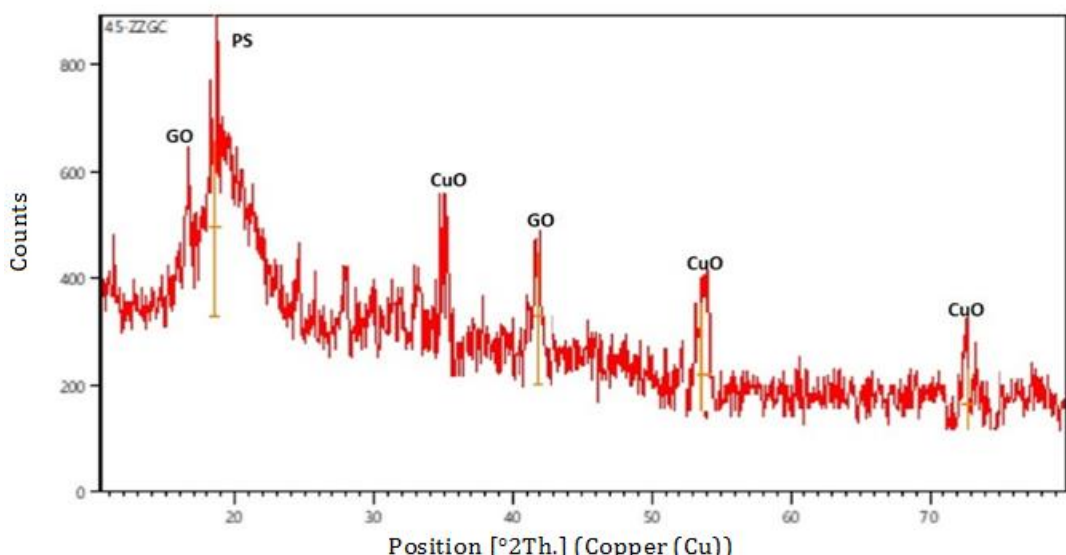


**Figure 2:** XRD pattern of PS/GO/CuO nanocomposites

In Figure 1 and Table 2, the X-ray diffraction pattern was demonstrated for PS/TiO<sub>2</sub>/CuO nanocomposites, the polymer diffraction peaks at  $2\theta = 19.0702^\circ$  and  $22.683^\circ$  corresponding to  $597.64^\circ$  and  $289.02^\circ$ , respectively, while it indicated the TiO<sub>2</sub> NPs diffraction peaks at  $2\theta = 25.41^\circ$ ,  $26.793^\circ$ ,  $48.034^\circ$ ,  $54.487^\circ$ , and  $69.729^\circ$  corresponding to 994.28, 774.58, 341.12, 170.57, and 52.72, respectively, compared with the standard reference for TiO<sub>2</sub> NPs [12]. Furthermore, XRD diffraction peaks for CuO NPs at  $2\theta =$  were  $32.155^\circ$ ,  $38.577^\circ$ ,  $45.947^\circ$ ,  $62.629^\circ$ , and  $75.808^\circ$  corresponding to 507.61, 209.52, 292.13, 122.24, and 61.98 compared with the standard reference for CuO NPs, as depicted in Figure 2 [13].

**Table 2:** XRD record of PS/TiO<sub>2</sub>/CuO nanocomposites

Pos. [°2Th.]	Height [cts]	FWHM Left [°2Th.]	Matched by	Particle size (nm)	Average particle size (nm)
19.0702	597.64	0.5904	Polymer	14.26	14.94
22.6835	289.02	0.5904	Polymer	14.34	
25.4150	994.28	0.2460	TiO <sub>2</sub> NPs	34.59	
26.7931	774.58	0.3444	TiO <sub>2</sub> NPs	24.78	
32.1553	507.61	0.3444	CuO NPs	25.08	
38.5770	209.52	0.9840	CuO NPs	8.94	
45.9472	292.13	0.4920	CuO NPs	18.33	
48.0347	341.12	0.7872	TiO <sub>2</sub> NPs	11.54	
54.4876	170.57	1.1808	TiO <sub>2</sub> NPs	7.91	
62.6294	122.24	0.9840	CuO NPs	9.88	
69.7299	52.72	2.3616	TiO <sub>2</sub> NPs	4.28	
75.8087	61.98	1.9680	CuO NPs	5.35	

*X-Ray diffraction of PS/GO/CuO nanocomposites*

**Figure 2** and **Table 3** illustrated the X-ray diffraction pattern for PS/TiO<sub>2</sub>/CuO nanocomposites, polystyrene diffraction peaks at  $2\theta = 18.5536^\circ$  corresponding to  $331.27^\circ$ , while XRD diffraction peaks for CuO NPs at  $2\theta = 35.1124^\circ$ ,  $53.9342^\circ$ , and  $72.9231^\circ$  corresponding to  $129.65^\circ$ ,  $226.23^\circ$ ,  $226.23^\circ$ , and  $233.54^\circ$ , respectively. Furthermore, graphene oxide NPs diffraction peaks at  $2\theta = 13.8112^\circ$  and  $42.0926^\circ$  corresponding to  $296.32^\circ$  and  $265.01^\circ$ , respectively [14].

*Thermogravimetric analysis of PS/TiO<sub>2</sub>/CuO nanocomposites*

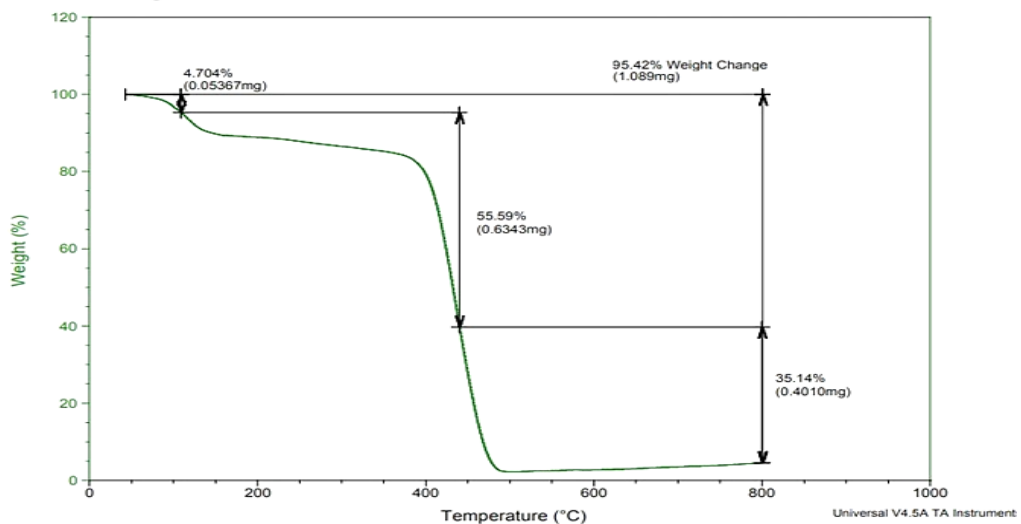
Thermogravimetric analysis of prepared nanocomposites is indicated in **Figure 3** in four stages of weight loss [15]:

The first stage: At  $35-120^\circ\text{C}$  with a weight loss percentage of 4.704% was attributed to the loss of water (absorbed from the atmosphere) which physically adsorbed the nanocomposite due to the fact that the nanomaterials have very high surface area.

The second stage: At  $120-440^\circ\text{C}$  and the third stage at  $440-800^\circ\text{C}$  with a total weight (percentage) loss equal to 95.42% (found) corresponding 83.3% (calculated), these stages include the starting of styrene unit loss and there is decomposition of the carbon skeleton of the polymer. The fourth stage: At temperature more than  $800^\circ\text{C}$  with weight (percentage) of 4.566% (found) corresponding 16.6% (calculated), this stage was attributed to the amount of TiO<sub>2</sub> and CuO NPs. We noticed that the weight loss at  $440^\circ\text{C}$  of PS/TiO<sub>2</sub>/CuO nanocomposites was more than that of PS/TiO<sub>2</sub>/Ag<sub>2</sub>O nanocomposites (**Table 4**).

**Table 3:** XRD record of PS/GO/CuO nanocomposites

Pos. [°2Th.]	Height [cts]	FWHM Left [°2Th.]	Matched by	Particle size (nm)	Average particle size (nm)
13.8112	296.32	0.2921	GO NPs	28.62	16.93
18.5536	331.27	0.5600	Polystyrene	15.02	
35.1124	129.65	0.4388	CuO NPs	19.84	
42.0926	265.01	0.6920	GO NPs	12.85	
53.9342	226.23	0.7632	CuO NPs	12.20	
72.9231	233.54	0.7911	CuO NPs	13.05	

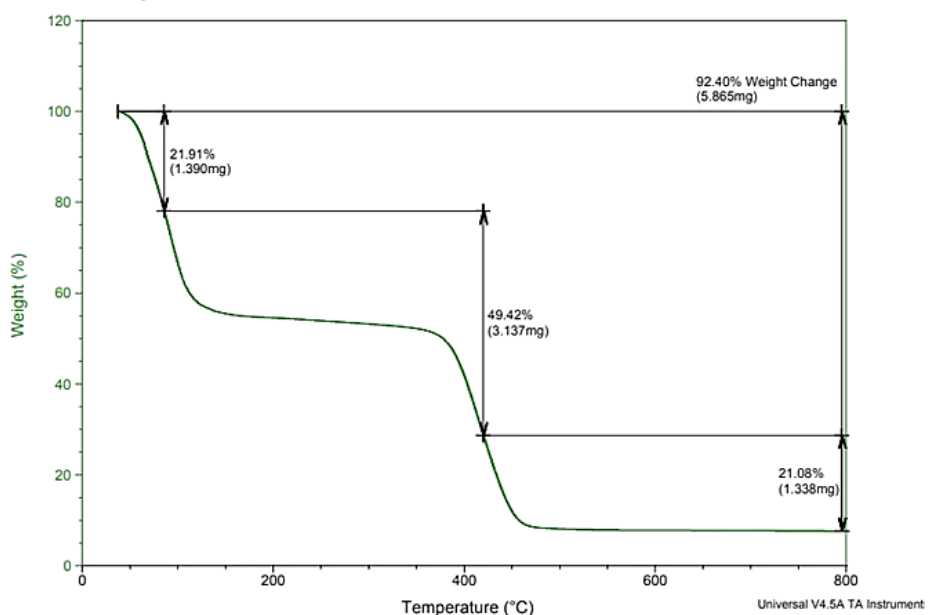
**Figure 3:** FA electronic spectrum**Table 4:** All stage decompositions for PS/TiO<sub>2</sub>/CuO nanocomposites

Ser.	Stage (temperature °C)	Loss wt%	Status
1	35-120	4.704	Loss of water
2	120-440	55.59	Starting of loss of styrene unit
3	440-800	35.14	Decomposition of carbon skeleton
4	More than 800	4.566	Metal and metal oxide residue

#### Thermogravimetric analysis of PS/GO/CuO nanocomposites

The graphene oxide nanocomposites were thermally decomposed as follows [16]: The first stage: at 35-120 °C with a weight loss percentage of 21.91% was attributed to the loss of water. The second stage: at 120-440 °C and the third stage at

440-800 °C with a total weight (percentage) loss equal to 92.40%, these stages include the starting of styrene unit loss and there is the decomposition of the carbon skeleton of the polymer. The fourth stage: at temperature than 800°C with weight (percentage) of 7.59%, this stage was attributed to the residue amount metal oxides NPs. See [Figure 4](#) and [Table 5](#).

**Figure 4:** TG analysis of PS/GO/CuO nanocomposites

**Table 5:** TG analysis of PS/GO/CuO nanocomposites

Ser.	Stage (temperature °C)	Loss wt%	Status
1	35-120	21.91	Loss of water
2	120-440	49.42	Starting of loss styrene unit
3	440-800	21.08	Decomposition of carbon skeleton
4	More than 800	7.59	Metal and metal oxide residue

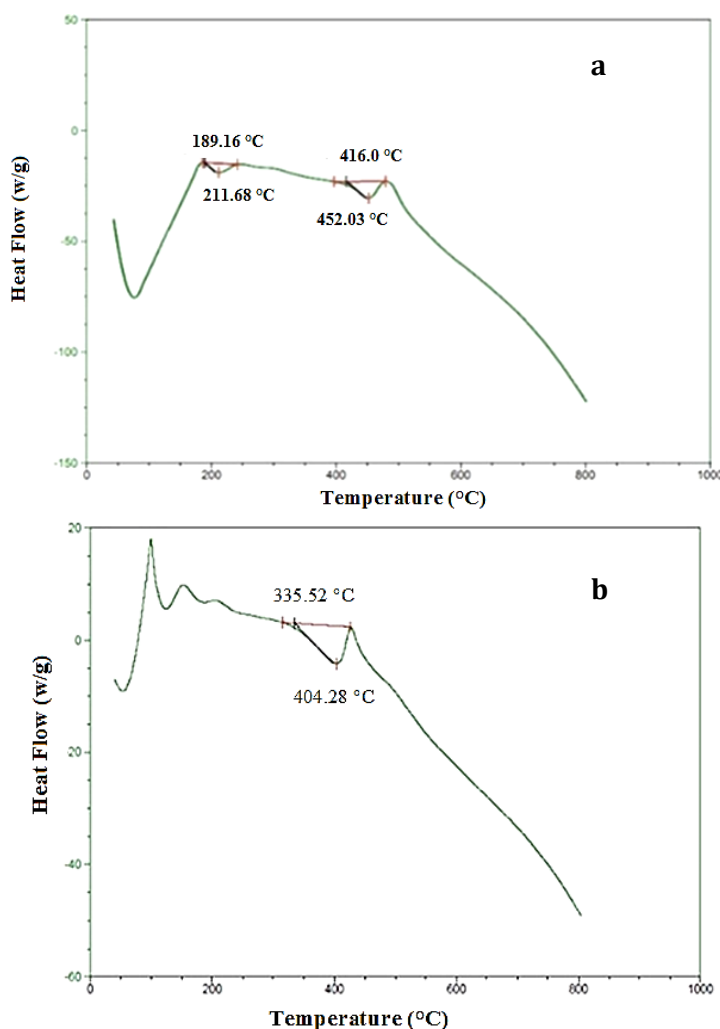
*Differential Scanning Calorimetry (DSC) of (PS/TiO<sub>2</sub>/CuO) nanocomposites*

Differential scanning calorimetry (DSC) analysis was done for the prepared PS/TiO<sub>2</sub>/CuO and PS/GO/CuO nanocomposites in two endothermic stages: First, at 211.68 °C equal ΔH to 350.9 J/g for PS/TiO<sub>2</sub>/CuO, at 335.52 °C equal ΔH to 1063 J/g for PS/GO/CuO. It is considered as a glass transition of polystyrene in nanocomposites compared with standard reference of polystyrene which is 100°C. Second, at 252.03 °C and 404.28 °C, respectively that were conceded melting point of polystyrene in nanocomposites compared with

the standard reference of polystyrene which is 270 °C [17], as displayed in [Figure 5](#).

*The field emission scanning electron microscopy (FE-SEM) of (PS/TiO<sub>2</sub>/CuO) nanocomposites*

The field emission scanning electron microscopy (FE-SEM) measurement indicates that there are two different nano structures, which are irregular sphere like nano structures with diameter range between 45.76-46.27 nm, sheet like nanoparticles with a thickness of approximately 40 nm, these nano structures means that the prepared nanocomposite is within the nanoscale [18] (See [Figure 6](#)).

**Figure 5:** DSC/TGA of a) PS/TiO<sub>2</sub>/CuO and b) PS/GO/CuO nanocomposites

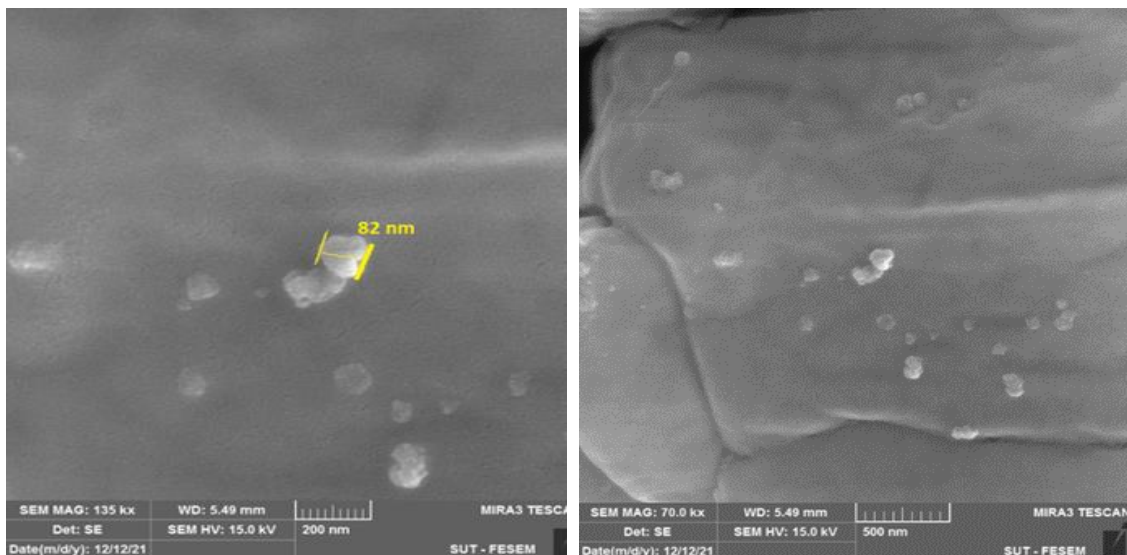


**Figure 6:** FE-SEM of PS/TiO<sub>2</sub>/CuO nanocomposites

#### The field emission scanning electron microscopy (FE-SEM) of PS/GO/CuO nanocomposites

The field emission scanning electron microscopy (FE-SEM) measurement of the PS/GO/CuO

nanocomposites showed that nanoparticles sizes are between 51.56-54.86 nm and this is within the nanoscale. The shape of these nanoparticles is spherical and semi-spherical, as exhibited in Figure 7 [19].

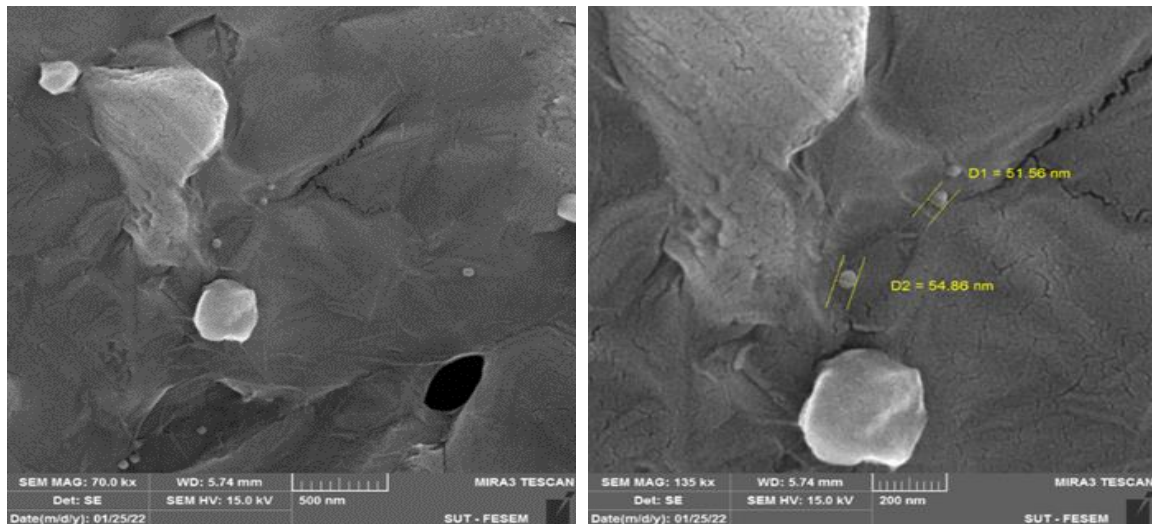


**Figure 7:** FE-SEM of PS/GO/CUO nanocomposites

#### Application

##### Antibacterial activity

The biological results on bacteria (*Klebsiella pneumoniae*) and (*Staphylococcus aureus*) illustrated that PS/TiO<sub>2</sub>/CuO and PS/GO/CuO nanocomposites have a different effect on inhibiting the growth of the studied bacteria, as presented in Table 6 and Figures 8 and 9. This is due to the ability of these nanocomposites to

production of free radicals, which leads to the oxidative stress, and thus damage to proteins, DNA, cell membranes, and binding to cytosolic proteins, DNA, and enzymes. This interaction causes decreased inhibiting respiratory chain, ATP production, and metabolic pathways [20, 21]. The nanocomposites disrupt the act of the bacterial cell membrane through electrostatic binding and release of positively charged metal ions vs. the negative charge of the cell membrane.

These charges interfere on the surface through electrostatic binding, which results in an increase in oxidative stress and damage occurs in the cell membrane [22].

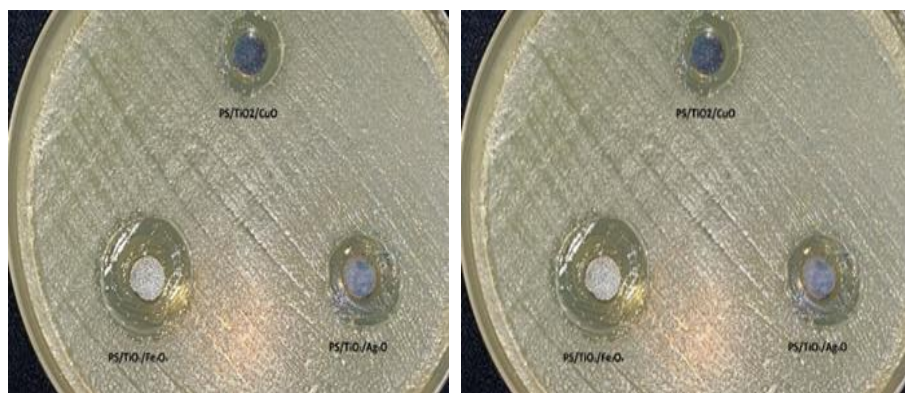
#### *Antifungal activity*

The anti-fungal activity of PS/TiO<sub>2</sub>/CuO and PS/GO/CuO nanocomposites synthesized by the

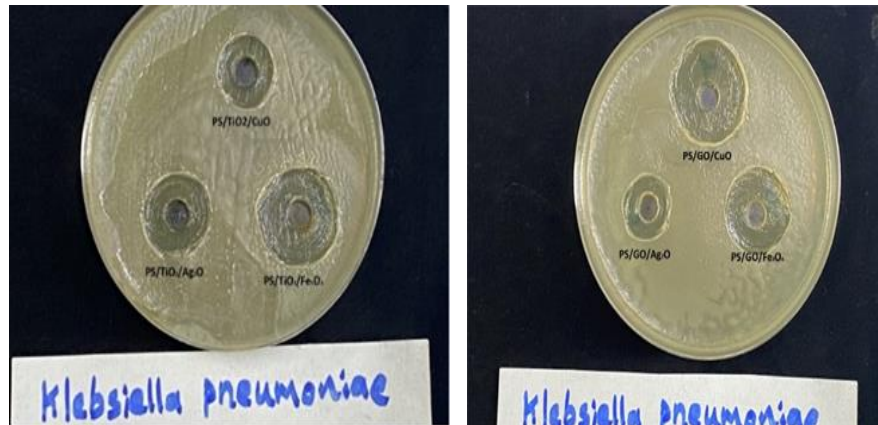
green and sol-gel method was studied on *Candida Albicans*, the results demonstrated that PS/GO/CuO nanocomposites gave the strongest anti-fungal activity against *Candida Albicans*. This is due to the increase in the surface area of the nanocomposite through the presence of graphene oxide and the small size of copper, which helps to penetrate the cell membrane [23]. (See Table 7 and Figure 10).

**Table 6:** Antibacterial susceptibility test

Ser.	Nanocompsites name	<i>Staphylococcus aureus</i> (+)	<i>Klebsiella</i> (-)
1	PS/TiO <sub>2</sub> /CuO	12 mm	17 mm
2	PS/GO/CuO	28 mm	26 mm



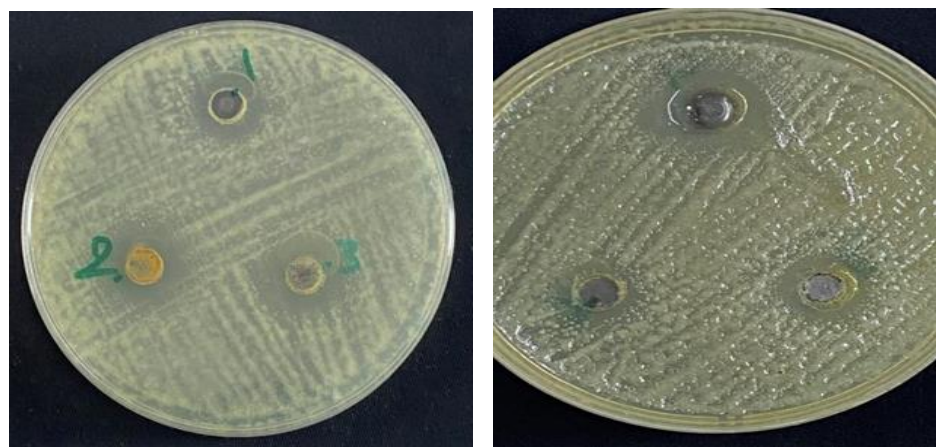
**Figure 8:** Biological test (*Staphylococcus aureus*) of PS/GO/Ag<sub>2</sub>O and PS/TiO<sub>2</sub>/Ag<sub>2</sub>O nanocomposites



**Figure 9:** Biological test (*Klebsiella*) of PS/GO/Ag<sub>2</sub>O and PS/TiO<sub>2</sub>/Ag<sub>2</sub>O nanocomposites

**Table 7:** Antibacterial susceptibility test

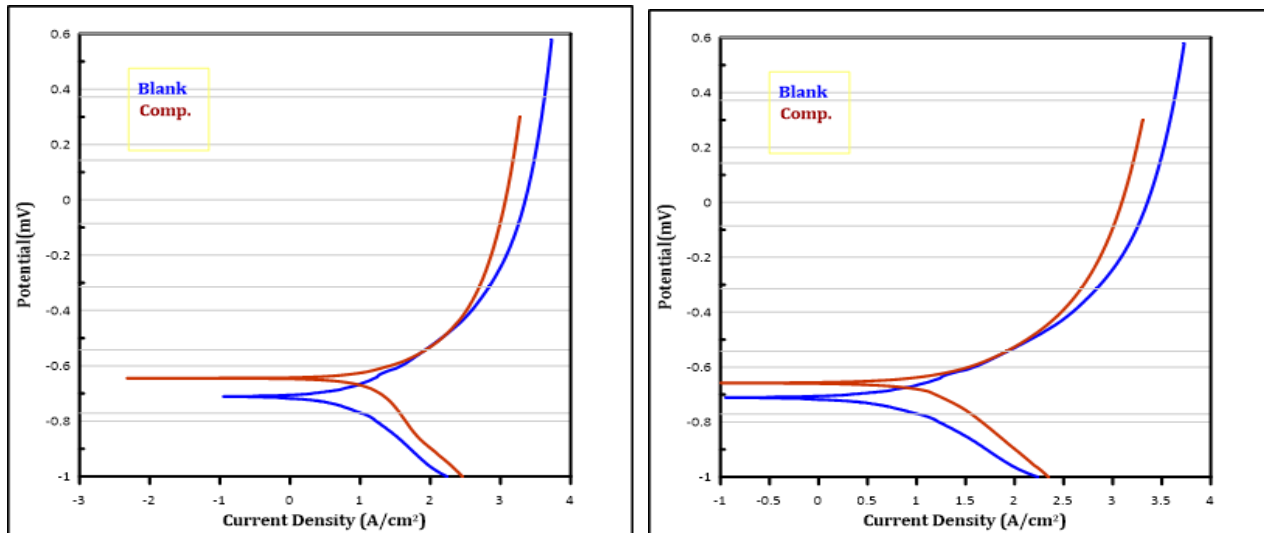
Ser.	Nanocompsites name	<i>Candida Albicans</i>
1	PS/TiO <sub>2</sub> /CuO	16 mm
2	PS/GO/CuO	21 mm

**Figure 10:** Biological test of *Candida albicans*

### Corrosion test

The corrosion records were measured and presented in the [Table 8](#) and [Figure 11](#). The measurements indicate that the synthesized nanocomposites gave different results and showed that the carbon steel coated with the synthetic nanocomposites had a high protection rate or inhibition efficiency (IE %) compared with

the uncoated carbon steel. The graphene oxides nanocomposites (PS+GO+CuO) gave a high protection rate of 92%, while the titanium dioxide nanocomposites (PS+TiO<sub>2</sub>+CuO), which amounted to 90%, the recorded also demonstrated an increase in the corrosion resistance value of carbon steel coated with synthetic nanocomposites compared with the used carbon steel [24].

**Figure 11:** Carbon steel uncoated, PS+TiO<sub>2</sub>+CuO, and PS/GO/CuO with carbon steel coated**Table 8:** Corrosion test

Comp.	<i>E corr.</i>	<i>I corr.</i>	<i>I corr./r</i>	Resistant	Anodic $\beta$	Cathodic $\beta$	Corr. rate	IE%
Blank	-0.998	146.4	1.464	523.8	0.950	0.217	0.718	-
PS+GO+CuO	-0.666	11.90	1.190E-5	3944	0.171	0.294	0.058	92
PS+TiO <sub>2</sub> +CuO	-0.646	15.21	1.521E-5	2816	0.140	0.332	0.075	90

## Conclusion

The nanoparticles synthesis by green methods is an inexpensive (economic) method and at the same time, it preserves the environment from pollution, while the nanoparticles synthesis from chemicals is costly and harmful to the environment. The results proved that the PS+TiO<sub>2</sub>+CuO and PS+GO+CuO nanocomposites studied by the X-ray diffraction and FE-SEM had the nanoparticles presence of different sizes, within the nanoscale, and the thermal analysis of the nanocomposites was measured and gave an improvement in the physical properties of polystyrene which is an increase in the melting point and glass transition. Biological applications were carried out on the nanocomposites, the tests were conducted on (*Staphylococcus aureus*) and (*Klebsiella*) bacteria, the PS+GO+CuO nanocomposite gave the highest inhibition than PS+TiO<sub>2</sub>+CuO. Furthermore, the antifungal activity was tested on *Candida parapsilosis*, the test also proved that the PS+GO+CuO nanocomposite is more inhibiting than PS+TiO<sub>2</sub>+CuO. The results of the anti-corrosion tests gave the protection ratio of PS+GO+CuO nanocomposite (92%) was higher than PS+TiO<sub>2</sub>+CuO (90%).

## Acknowledgements

This research was supported by Dr. Nada Mutter Abbass, university of Baghdad, college of science, department of chemistry. We thank our colleagues who provided insight and expertise that assisted the research. We also do not forget to support the family.

## Funding

This research did not receive any specific grant from funding agencies in the public, commercial, or not-for-profit sectors.

## Authors' contributions

All authors contributed to data analysis, drafting, and revising of the paper and agreed to be responsible for all the aspects of this work.

## Conflict of Interest

There are no conflicts of interest in this study.

## ORCID:

Zeyad Zaid Almarbd

<https://www.orcid.org/0000-0002-9771-5517>

## References

- [1]. Bayda S., Adeel M., Tuccinardi T., Cordani M., Rizzolio F., The History of Nanoscience and Nanotechnology: From Chemical-Physical Applications to Nanomedicine, *Molecules*, 2020, **25**:112 [[Crossref](#)], [[Google Scholar](#)], [[Publisher](#)]
- [2]. Termonia Y., Chain Confinement in Polymer Nanocomposites and Its Effect on Polymer Bulk Properties, *Journal of Polymer Science Part B: Polymer Physics*, 2010, **48**:687 [[Crossref](#)], [[Google Scholar](#)], [[Publisher](#)]
- [3]. Kadham A.J., Hassan D., Mohammad N., Ah-yanari A.H., Fabrication of (Polymer Blend-magnesium Oxide) Nanoparticle and Studying their Optical Properties for Optoelectronic Applications, *Bulletin of Electrical Engineering and Informatics (BEEI)*, 2018, **7**:28 [[Crossref](#)], [[Google Scholar](#)], [[Publisher](#)]
- [4]. Macwan D.P., Dave P.N., Chaturvedi S., A review on nano-TiO<sub>2</sub> sol-gel type syntheses and its applications, *Journal of Materials Science*, 2011, **46**:3669 [[Crossref](#)], [[Google Scholar](#)], [[Publisher](#)]
- [5]. Singh J., Dutta T., Kim K.H., Rawat M., Samddar P., Kumar P., Green Synthesis of Metals and Their Oxide Nanoparticles: Applications for Environmental Remediation, *Journal of nanobiotechnology*, 2018, **16**:84 [[Crossref](#)], [[Google Scholar](#)], [[Publisher](#)]
- [6]. El-Ansary A., Warsy A., Daghestani M., Merghani N.M., Al-Dbass A., Bukhari W., Al-Ojayan B., Ibrahim E.M., Al-Qahtani A.M., Bhat R.S., Characterization, antibacterial and neurotoxic effect of Green synthesized nanosilver using *Ziziphus spina Christi* aqueous leaf extract collected from Riyadh, Saudi Arabia, *Materials Research Express*, 2018, **5**:025033 [[Crossref](#)], [[Google Scholar](#)], [[Publisher](#)]
- [7]. Khani R., Roostaei B., Bagherzade G., Moudi M., Green synthesis of copper nanoparticles by fruit extract of *Ziziphus spina-christi* (L.) Willd.: [Page 950]

- application for adsorption of triphenylmethane dye and antibacterial assay, *Journal of Molecular Liquids*, 2018, **255**:541 [[Crossref](#)], [[Google Scholar](#)], [[Publisher](#)]
- [8]. Dubey R.S., Krishnamurthy K.V., Singh S., Experimental studies of TiO<sub>2</sub> nanoparticles synthesized by solgel and solvothermal routes for DSSCs application, *Results in Physics*, 2019, **14**:102390 [[Crossref](#)], [[Google Scholar](#)], [[Publisher](#)]
- [9]. Paulchamy B., Arthi G., Lignesh B.D., A simple approach to stepwise synthesis of graphene oxide nanomedicine & nanotechnology, *Journal of Nanomedicine & Nanotechnology*, 2015, **6**:1 [[Crossref](#)], [[Google Scholar](#)], [[Publisher](#)]
- [10]. Ahmad W., Ahmad Q., Yaseen M., Ahmad I., Hussain F., Mohamed Jan B., Ikram R., Stylianakis M.M., Kenanakis G., Development of Waste Polystyrene-Based Copper Oxide/Reduced Graphene Oxide Composites and Their Mechanical, Electrical and Thermal Properties, *Nanomaterials*, 2021, **11**:2327 [[Crossref](#)], [[Google Scholar](#)], [[Publisher](#)]
- [11]. Chaudhary R.G., Bhusari G.S., Tiple A.D., Rai A.R., Somkuvar S.R., Potbhare A.K., Lambat T.L., Ingle P.P., Abdala A.A., Metal/Metal Oxide Nanoparticles: Toxicity, Applications, and Future Prospects, *Current Pharmaceutical Design*, 2019, **25**:4013 [[Crossref](#)], [[Google Scholar](#)], [[Publisher](#)]
- [12]. Teng T.P., Teng T.C., Pan S.I., Degradation of Gaseous Formaldehyde by Visible Light-Responsive Titania Photocatalyst Filter, *International Journal of Photoenergy*, 2012, **2012**:739734 [[Crossref](#)], [[Google Scholar](#)], [[Publisher](#)].
- [13]. Suresh S., Karthikeyan S., Jayamoorthy K., FTIR and multivariate analysis to study the effect of bulk and nano copper oxide on peanut plant leaves, *Journal of Science: Advanced Materials and Devices*, 2016, **1**:343 [[Crossref](#)], [[Google Scholar](#)], [[Publisher](#)]
- [14]. Siburian R., Sihotang H., Raja S.L., Supeno M., Simanjuntak C., New Route to Synthesize of Graphene Nano Sheets, *Asian Journal of Chemistry*, 2018, **34**:182 [[Crossref](#)], [[Google Scholar](#)], [[Publisher](#)]
- [15]. Farha A.H., Al Naim A.F., Mansour S.A., Thermal Degradation of Polystyrene (PS) Nanocomposites Loaded with Sol Gel-Synthesized ZnO Nanorods, *Polymers*, 2020, **12**:1935 [[Crossref](#)], [[Google Scholar](#)], [[Publisher](#)]
- [16]. Li C., Lu Y., Yu W., Zhao R., Du S., Ke N., Self-assembly preparation and thermal decomposition of Al/CuO/graphene oxide, *IOP Conference Series: Earth and Environmental Science*, 2021, **680**:012081 [[Crossref](#)], [[Google Scholar](#)], [[Publisher](#)]
- [17]. Panwar A., Choudhary V., Sharma D.K., Role of compatibilizer and processing method on the mechanical, thermal and barrier properties of polystyrene/organoclay nanocomposites, *Journal of Reinforced Plastics and Composites*, 2013, **32**:740 [[Crossref](#)], [[Google Scholar](#)], [[Publisher](#)]
- [18]. Ratnawulan R., Ramli R., Fauzi A., Hayati AE S., Synthesis and Characterization of Polystyrene/CuO-Fe<sub>2</sub>O<sub>3</sub> Nanocomposites from Natural Materials as Hydrophobic Photocatalytic Coatings, *Crystals*, 2021, **11**:31 [[Crossref](#)], [[Google Scholar](#)], [[Publisher](#)]
- [19]. Gupta A., Jamatia R., Patil R.A., Ma Y.R., Pal A.K., Copper Oxide/Reduced Graphene Oxide Nanocomposite-Catalyzed Synthesis of Flavanones and Flavanones with Triazole Hybrid Molecules in One Pot: A Green and Sustainable Approach, *ACS Omega*, 2018, **3**:7288 [[Crossref](#)], [[Google Scholar](#)], [[Publisher](#)]
- [20]. Moghaddam A., Zamani H., Karimi-Maleh H., A New Sensing Strategy for Determination of Tamoxifen Using Fe3O4/Graphene-Ionic Liquid Nanocomposite Amplified Paste Electrode, *Chemical Methodologies*, 2021, **5**:373 [[Crossref](#)], [[Google Scholar](#)], [[Publisher](#)]
- [21]. Morones J.R., Elechiguerra J.L., Camacho A., Holt K., Kouri J.B., Ramírez J.T., Yacaman M.J., The bactericidal effect of silver nanoparticles, *Nanotechnology*, 2005, **16**:2346 [[Crossref](#)], [[Google Scholar](#)], [[Publisher](#)]
- [22]. Kim J.S., Kuk E., Yu K.N., Kim J.H., Park S.J., Lee H.J., Kim S.H., Park Y.K., Park Y.H., Hwang C.Y., Kim Y.K., Lee Y.S., Jeong D.H., Cho M.H., Antimicrobial effects of silver nanoparticles, *Nanomedicine*, 2017, **3**:95 [[Crossref](#)], [[Google Scholar](#)], [[Publisher](#)]
- [23]. Kim K.J., Sung W.S., Suh B.K., Moon S.K., Choi J.S., Kim J.G., Lee D.G., Antifungal activity and mode of action of silver nano-particles on Candida

albicans, *Biometals*, 2009, 22:235 [[Crossref](#)], [[Google Scholar](#)], [[Publisher](#)]  
[24]. Girciene O., Ramanauskas K., Gudaviciute L., Martusiené A., The effect of phosphate coatings on carbon steel protection from corrosion in a chloride contaminated alkaline solution, *Chemia*, 2013, 24:251 [[Google Scholar](#)], [[Publisher](#)]

### HOW TO CITE THIS ARTICLE

Zeyad Zaid Almarbd, Nada Mutter Abbass. Recycling of plastic waste made of polystyrene and its transformation into nanocomposites by green methods. *Chem. Methodol.*, 2022, 6(12) 940-952  
<https://doi.org/10.22034/CHEMM.2022.359620.1603>  
URL: [http://www.chemmethod.com/article\\_156148.html](http://www.chemmethod.com/article_156148.html)